Nonradiative Carrier Recombination Enhanced by Vacancy Defects in Ionic *II-VI* Semiconductors

Dan Guo,[1,2] Chen Qiu,[1] Kaike Yang,[3] and Hui-Xiong Deng[1,2,*]

[1] *State Key Laboratory of Superlattices and Microstructures, Institute of Semiconductors, Chinese Academy of Sciences, Beijing 100083, China*

[2] *Center of Materials Science and Optoelectronics Engineering, University of Chinese Academy of Sciences, Beijing 100049, China*

[3] *Key Laboratory of Low-Dimensional Quantum Structures and Quantum Control of Ministry of Education, Synergetic Innovation Center for Quantum Effects and Applications, Department of Physics, Hunan Normal University, Changsha 410081, China*

(Received 15 March 2021; revised 10 May 2021; accepted 17 May 2021; published 10 June 2021)

Nonradiative-recombination-related defects are significant for optoelectronic semiconductor devices. Here, we analyze nonradiative-recombination processes in ionic semiconductors using first-principles density-functional theory. In ionic group II-VI semiconductors, we find that large lattice relaxations of anion vacancies caused by strong Coulomb interactions between different charged defect states can significantly enhance recombination processes through a two-level recombination mechanism. Specifically, we show that the defect level of the 2+ charged anion vacancy (V_{Se}^{2+}) in group II-VI ZnSe is close to the conduction-band minimum and easily captures an electron to form a metastable 1+ charged state (V_{Se}^{+}); then, the large lattice relaxation, on account of the change in Coulomb interactions locally in the different charged states, rapidly changes this metastable state to a stable one and simultaneously move the defect level of V_{Se}^{+} closer to that valence-band maximum, and thus, increases the hole-capture rate. Compared with the Shockley-Read-Hall nonradiative-recombination theory based on a single defect level, this two-level recombination mechanism involving anion vacancies can greatly increase the nonradiative-recombination rate in ionic group II-VI semiconductors. This understanding is expected to be useful for the study of the nonradiative-recombination process in ionic semiconductors for applications in the field of optoelectronic devices.

DOI: 10.1103/PhysRevApplied.15.064025

I. INTRODUCTION

Nonradiative carrier recombination plays an important role in researching semiconductor materials. It is often known as Shockley-Read-Hall (SRH) recombination [1–3]. Nonradiative recombination will reduce device efficiencies through suppressing luminescence and decreasing photogenerated carriers or carrier lifetimes in the field of optoelectronic devices [4,5]. In defect-induced nonradiative recombination, a defect level first traps an electron (hole) with the help of phonons and then traps a hole (electron), resulting in carrier recombination. Generally speaking, electrons can be more easily trapped by a defect level that is close to the conduction-band minimum (CBM), but it will be difficult for holes to be trapped. For the same reason, a defect level close to the valence-band maximum (VBM) can trap holes easily and is difficult to trap electrons [6–8]. Hence, the recombination process is decided by the slower step of the trapping rate of the electron or hole. Accordingly, defect levels near the middle of the band gap in a material should be considered as the most important recombination centers.

Covalent semiconductors, such as silicon and germanium, usually have relatively deep intrinsic defect levels compared with ionic semiconductors [9–11]. In covalent semiconductors, the dangling-bond states are close to the middle of the band gap, thus the defect levels are deep. However, the dangling-bond states are near to the band edges for ionic semiconductors; therefore, the defect levels are shallow [12,13]. Based on the conventional SRH model, ionic semiconductors should possess lower carrier capture rates than covalent semiconductors. However, experimental results show that the carrier capture coefficient measured for ionic group II-VI semiconductors is higher than that in silicon. For example, in the ZnO crystal, the hole-capture rate resulting from intrinsic defects measured experimentally reaches 3×10^{-7} cm^3/s [14]. Unexpectedly, the hole-capture rate determined experimentally in silicon is only 1×10^{-9} cm^3/s [15]. This

*hxdeng@semi.ac.cn

is in contradiction with the SRH model, and the physical origin is unclear.

To understand why ionic semiconductors have larger nonradiative-recombination rates, we take the ZnSe crystal as a representative example to investigate the nonradiative-recombination process in group II-VI ionic semiconductors. By using first-principles method, we investigate the intrinsic defect properties and densities of defects in different charge states of bulk ZnSe. Through employing static coupling theory [6,16–19], we carefully calculate the nonradiative-recombination rate and analyze the recombination process through the intrinsic defects in ZnSe. We find that the 2+ charged selenium vacancy (V_{Se}^{2+}) in ZnSe exhibits a large lattice structure relaxation caused by strong Coulomb interactions between the nearest zinc atoms to the vacancy. The defect level of V_{Se}^{2+} in ZnSe is close to the conduction band and easily captures an electron to form metastable V_{Se}^{+}. Then, the large lattice relaxation resulting from the Coulomb interactions rapidly transforms the metastable state into a stable one, and simultaneously moves the defect level of V_{Se}^{+} closer to the valence band, and thus, increases the hole-capture rate. Therefore, the defect level that is close to the valence band can trap a hole at a high rate, and the electron can be trapped by the other defect level near the conduction band at a high rate as well. Consequently, the nonradiative-recombination process through this two-level mechanism can be enhanced in ionic group II-VI semiconductors.

II. METHODS

Our first-principles calculations of total energy and electronic structure are performed by density-functional theory (DFT), as implemented in the PWmat code [18,20], with the pseudopotentials that adopt the NCPP-SG15-PBE [21–23]. To improve the accuracy of the band gap, the Heyd-Scuseria-Ernzerhof (HSE06) [24] hybrid functional method by mixing with 38% of the Hartree-Fock term is employed. The calculated lattice constant of perfect ZnSe is 5.69 Å with a band gap of 2.68 eV, which is in good agreement with experiments [25]. A 64-atom supercell is used in all defect calculations. The convergence with the supercell size is checked carefully until a 216-atom supercell, and the effect of cell-cell Coulomb interactions for charged systems can be ignored. The convergence of the plane-wave cutoff energy and the Monkhorst-Pack k-point grid in the Brillouin zone [26] is examined carefully. All atoms within the supercell are fully relaxed until the forces on each atom are less than 0.01 eV/Å. The total energies are calculated with $3 \times 3 \times 3$ Monkhorst-Pack special k-point meshes. The convergence threshold of the total energy is less than 10^{-4} eV using an energy cutoff of 60 Ry. The defect-formation energy $\Delta H_f(\alpha, q)$ of defect α at charge state q and the defect transition level are determined according to Refs. [27,28]:

$$\Delta H_f(\alpha, q) = E(\alpha, q) - E(\mathrm{host}) + \sum n_i(E_i + \mu_i) + q\varepsilon_{\mathrm{VBM}}(\mathrm{host}) + qE_F, \quad (1)$$

where μ_i is the chemical potential of constituent i, and E_i denotes the energy of the elemental solid or gas; $\varepsilon_{\mathrm{VBM}}(\mathrm{host})$ is the VBM energy of the host. n_i represents the number of atoms removed from the supercell to form defects, and q describes the number of electrons transferred from the supercell to the Fermi reservoirs. The defect-transition-energy level $\varepsilon(q/q')$ is the Fermi level, E_F, at which the formation energy for defect α at charge state q is equal to that at charge state q':

$$\varepsilon(q/q') = [\Delta E(\alpha, q) - \Delta E(\alpha, q')]/(q' - q). \quad (2)$$

The chemical potentials μ_i depend on the experimental growth conditions. To avoid precipitation of Zn and Se, μ_i are limited by $\mu_{\mathrm{Zn}} \leq 0$ and $\mu_{\mathrm{Se}} \leq 0$. To maintain a stable ZnSe compound, μ_i should also satisfy

$$\mu_{\mathrm{Zn}} + \mu_{\mathrm{Se}} = \Delta H_f(\mathrm{ZnSe}), \quad (3)$$

where $\Delta H_f(\mathrm{ZnSe})$ is the formation energy of bulk ZnSe. The calculated value is $\Delta H_f(\mathrm{ZnSe}) = -2.19$ eV. We can define the Zn-rich condition limit by $\mu_{\mathrm{Zn}} = 0$ and $\mu_{\mathrm{Se}} = -2.19$ eV. The Se-rich condition limit can be defined by $\mu_{\mathrm{Se}} = 0$ and $\mu_{\mathrm{Zn}} = -2.19$ eV.

The functional relationship between the density of charged defects and E_F can be determined by calculating the formation energy of charged defects, $\Delta H_f(\alpha, q)$. The concentrations of thermally excited electrons and holes at a given temperature can be calculated by using the formula presented in Ref. [29], in which the effective masses of electrons and holes adopt the experimental values. For ZnSe, the effective mass of the electron is $m_n^* = 0.16m_0$, and the effective mass of the hole is $m_p^* = 0.75m_0$, where m_0 is the electron mass [30,31]. Depending on the freezing-in approximation [32], once defects are formed at a high temperature, their densities can be retained after reducing the temperature and only different charge states of the same defects can redistribute accordingly [8,33]. Combining the neutralization condition in a semiconductor with defects, the Fermi energy, carrier densities, and defect densities with different charge states after the material is quenched can be obtained through solving equations self-consistently [8].

The electron-phonon coupling constant can be calculated within one self-consistent field calculation through the method reported by Shi *et al.* [6,16,18] based on static approximations [34,35]. The nonradiative decay probability, W_{ij}, between the initial electronic state i and the final

electronic state j is given by the conventional Fermi golden rule:

$$W_{ij} = \frac{2\pi}{\hbar}\sum_n\sum_m p(i,n)|V_{in,jm}|^2\delta(E_{in}-E_{jm}), \quad (4)$$

where $V_{in,jm}$ are the off-diagonal matrix elements of the electronic Hamiltonian, which defined as

$$V_{in,jm} = \langle\Psi_{j,m}(r,R)|H|\Psi_{i,n}(r,R)\rangle, \quad (5)$$

and $p(i,n)$ is the probability that the system is in the initial phonon state, $\Psi_{i,n}(r,R)$, so that $\sum_n p(i,n) = 1$. If the vibrational equilibrium rate considerably exceeds the nonradiative decay rate, $p(i,n)$ can be described by the Boltzmann distribution:

$$p(i,n) = Z^{-1}\exp(-\beta E_{in}), \quad (6)$$

where $Z = \sum_n \exp(-\beta E_{in})$ is the partition function and $\beta = (k_B T)^{-1}$. Under static coupling theory [34,35], the off-diagonal matrix elements $V_{in,jm}$ can be written as

$$\begin{aligned}\langle\Psi_{j,m}(r,R)|H|\Psi_{i,n}(r,R)\rangle &= \langle\psi_j(r,R_a)\varphi_{j,m}(R)|H_a \\ &+ \sum_k \frac{\partial H}{\partial Q_k}(Q_k - Q_{k,a})|\psi_i(r,R_a)\varphi_{i,n}(R)\rangle \\ &= \sum_k \langle\psi_j(r,R_a)|\frac{\partial H}{\partial Q_k}|\psi_i(r,R_a)\rangle \\ &\langle\varphi_{i,n}(R)|Q_k - Q_{k,a}|\varphi_{j,m}(R)\rangle \\ &= \sum_k C^k_{i,j}\cdot\langle\varphi_{i,n}(R)|\boldsymbol{Q_k}|\varphi_{j,m}(R)\rangle, \end{aligned} \quad (7)$$

where R_a is the relaxed atomic position of state i or j and $Q_{k,a}$ is normal phonon mode of electronic state i or j. The atomic vibration for the phonon state k is defined as $\mathbf{Q}_k \equiv Q_k - Q_{k,a}$, which can be calculated for electronic state i or j as

$$\mathbf{Q}_{(i,j)k} = \frac{1}{\sqrt{M_k}}\sum_R M_R\mu_k(R)R_{i,j}. \quad (8)$$

The electron-phonon coupling constant between electronic states i and j, as well as phonon mode k, can be written as

$$\begin{aligned}C^k_{i,j} &= \langle\psi_j(r,R_a)|\frac{\partial H}{\partial Q_k}|\psi_i(r,R_a)\rangle \\ &= \sum_R \mu_k(R)\langle\psi_j|\frac{\partial H}{\partial R}|\psi_i\rangle. \end{aligned} \quad (9)$$

To use *ab initio* methods to calculate the electron-phonon coupling, Wang *et al.* proposed a formula based on the static coupling approximation and Huang's work [36], known as Huang's formula [18],

$$W_{ij} = \left(\frac{\pi kT}{\lambda}\right)^{1/2}\left(\sum_k \frac{1}{\omega_k^2}|C^k_{i,j}|^2\right) exp \left[-\frac{(E_i - E_j - \lambda)^2}{4kT\lambda}\right], \quad (10)$$

where $\lambda = \sum_k |\Delta Q_{(i,j)k}|^2(\omega_k^2)/2$ is the reorganization energy (atomic relaxation energy after the transition between electronic states i and j). ω_k is the frequency of the kth harmonic phonon mode. After calculating the nonradiative decay probability, W_{ij}, the carrier-capture-rate coefficient can be obtained by $B = W_{ij}V$, where V is the volume of the supercell. The calculation procedure for the nonradiative-decay-probability rate is implemented within the PWmat code package [20].

III. RESULTS AND DISCUSSION

To study the nonradiative-recombination process induced by native defects in group II-VI ionic semiconductors, we take the ZnSe crystal as a representative example to calculate the nonradiative-recombination coefficient. We first calculate the defect-formation energies and the transition-energy levels of all of the basic native point defects in bulk ZnSe: Zn vacancy (V_{Zn}), Se vacancy (V_{Se}), Zn interstitial (Zn_i), Se interstitial (Se_i), and Zn_{Se} and Se_{Zn} antisites. Interstitial energies are calculated at two tetrahedral interstitial sites in ZnSe. One site (T_{Zn}) is tetrahedrally surrounded by four Zn atoms, while the other site (T_{Se}) is surrounded by four Se atoms. The calculated formation energies of the intrinsic defect as a function of the Fermi levels in bulk ZnSe under Zn-rich and Se-rich growth conditions are shown in Fig. 1. On account of the formation energies of Se_i at the T_{Zn} site for each charge state being smaller than that of Se_i at the T_{Se} site, we show only the formation energies of Se_i at the T_{Zn} site in Fig. 1, which agrees with Ref. [37]. One of the requirements of being an effective recombination center is that a defect should have a defect level close to the CBM when it traps an electron or has a defect level close to the VBM when it traps a hole. Because the capture rate of trapping more than one carrier is usually very small, we do not discuss such cases here. In our calculations, we find that the (+/2+) transition-energy level of V_{Se}^{2+} is 0.03 eV below the CBM, the (0/+) transition-energy level of $Zn_i^0(T_{Zn})$ is 0.37 eV below the CBM, the (0/+) transition-energy level of Se_{Zn}^+ is 0.59 eV below the CBM, and the (0/−) transition energy level of V_{Zn}^- is 0.11 eV above the VBM. Among them, V_{Se}^{2+}, $Zn_i^0(T_{Zn})$, and Se_{Zn}^+ are shallow donors, and thus, it may be easier to capture an electron from the conduction band. V_{Zn}^-

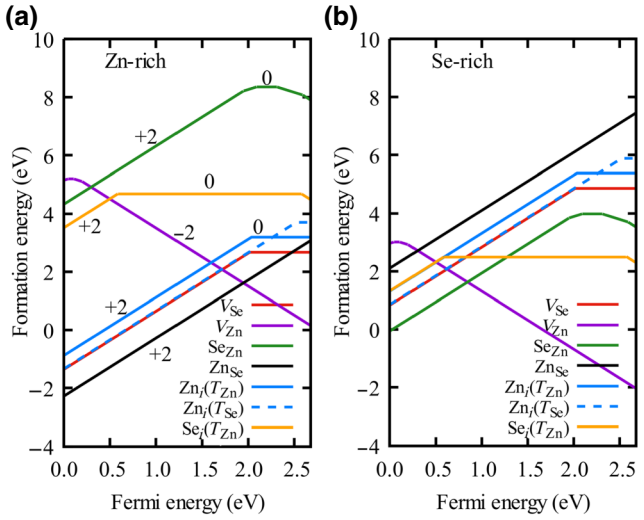

FIG. 1. Intrinsic defect-formation energies as a function of Fermi levels in ZnSe under (a) Zn-rich conditions and (b) Se-rich conditions.

is a shallow acceptor, and it may be easier to trap a hole from the valence band.

To obtain more accurate defect information on intrinsic ZnSe, we carry out thermodynamic simulations by considering all intrinsic defects in ZnSe under equilibrium growth conditions and after quenching. Figure 2(a) shows the defect densities as a function of zinc chemical potentials at a typical growth temperature at 1400 K [25,38]. After quenching to a working temperature of 300 K, the defect densities as a function of zinc chemical potential are shown in Fig. 2(b). The nonradiative-recombination center should also have significant defect densities. Although the defect densities of Zn_{Se}^{2+} and V_{Zn}^{2-} are extremely high, the (2+/+) transition-energy level of Zn_{Se}^{2+} is above the CBM. Thus, the defect level finds it very difficult to trap a hole from the valence band and cannot be an effective recombination center. The (2−/−) transition-energy level of V_{Zn}^{2-} is only 0.20 eV above the VBM. V_{Zn}^{2-} can trap a hole from the valence band easily and become V_{Zn}^{-}; however, V_{Zn}^{-} finds it very difficult to trap an electron from the conduction band because the defect level of V_{Zn}^{-} is far away from the conduction band. The calculated electron-capture-rate coefficient of V_{Zn}^{-} is $B_n = 1.0 \times 10^{-15}$ cm^{3}s^{-1}, which is too low to be an effective recombination center. Considering this, only V_{Se} has both shallow transition-energy levels and significant densities at the working temperature, and thus, may become an effective recombination center. In addition, under Zn-rich conditions, the calculated formation energy of V_{Se}^{0} is 2.67 eV, which is consistent with the value of 2.70 eV in Ref. [39].

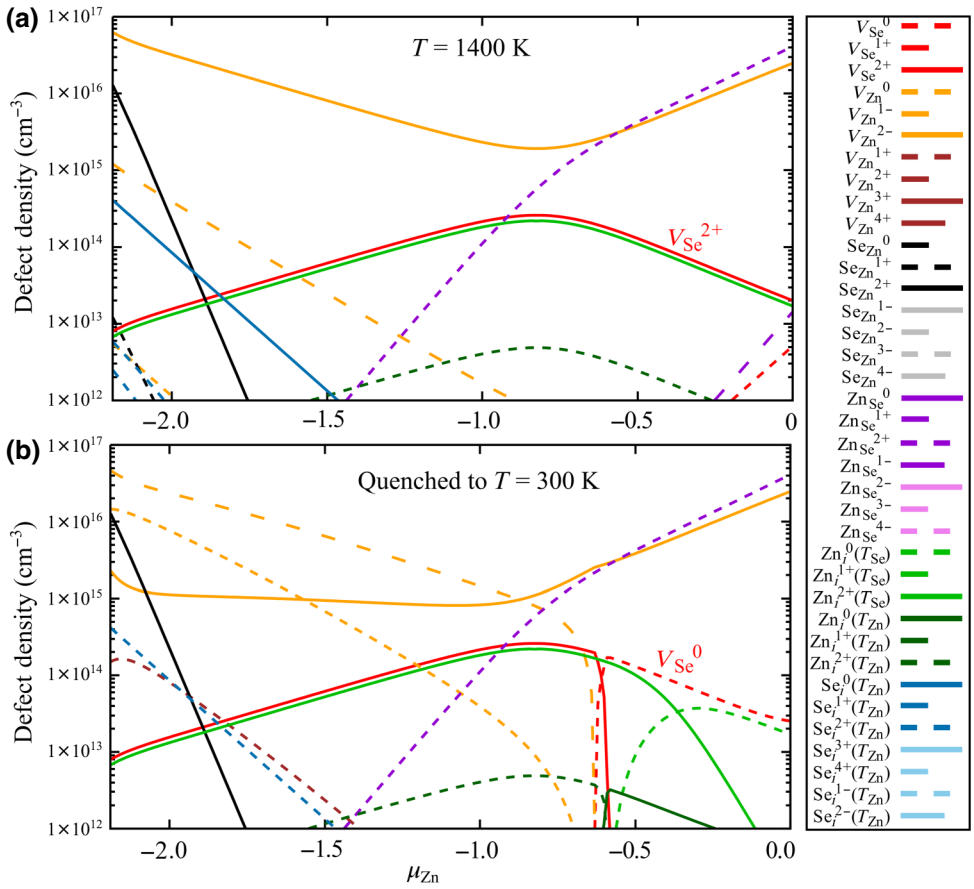

FIG. 2. (a) Defect density as a function of zinc chemical potential under thermodynamic equilibrium growth conditions at 1400 K. (b) Quenched (to 300 K) defect density as a function of zinc chemical potential.

The structure of V_{Se} has local C_{2v} symmetry, and its defect states consist of dangling bonds on the nearest-neighboring zinc atoms, induce a single state with a_1 symmetry in the band gap, and are fully occupied by two electrons. It is found that the Se vacancy in ZnSe exhibits a very large lattice distortion when it is 2+ charged (V_{Se}^{2+}). The large structure relaxation around the vacancy is very similar to that of V_{As}^{3+} in GaAs and V_O^{2+} in ZnO [40,41]. As shown in Fig. 3, for V_{Se}^0, four nearest zinc atoms move inward by 13.3% of the equilibrium Zn—O bond length; however, for V_{Se}^+ and V_{Se}^{2+}, the nearest-neighbors are moving outward by 10.2% and 24.3%, respectively. For V_{Se}^0, when the four nearest Zn atoms approach each other, the energy of the a_1 state is reduced and lies near the valence band, as shown in Fig. 3(c). For V_{Se}^+, the defect level is half occupied by one electron, and the four nearest Zn atoms move outward due to Coulomb interactions in the ionic group II-VI semiconductors, pushing the defect level upward to the middle of the band gap. In the V_{Se}^{2+} configuration, the defect level is unoccupied and the nearest-neighboring Zn atoms move outward significantly due to the larger Coulomb interactions, and the defect level is pushed near the CBM. A large decrease of the defect-formation energy is found due to the large lattice relaxation, making the Se vacancy a negative-U center, which is qualitatively consistent with Ref. [39].

When ZnSe grows under the condition of $\mu_{Zn} = -0.63$ eV, the Se vacancy is mainly in the 2+ charge state and possesses a high defect density of 1.96×10^{14} cm^{-3}, as shown in Fig. 2(b). By carefully considering the defect transition-energy levels related to V_{Se}^{2+} during trapping processes, we identify that nonradiative recombination caused by V_{Se}^{2+} can involve possible defects at points A and B, as shown in Fig. 4. For each trapping process, we

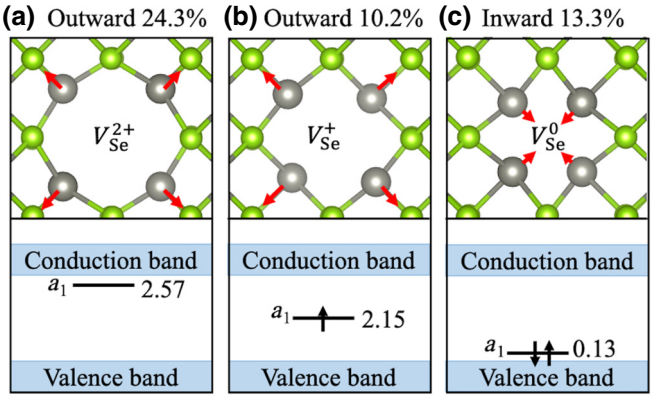

FIG. 3. Ball-and-stick representations of local atomic relaxations around the selenium vacancy in the 2+, 1+, and neutral charged states. Single-particle-level energies, with reference to the VBM, are also shown for each charge state. Green balls are Se atoms and gray balls are Zn atoms.

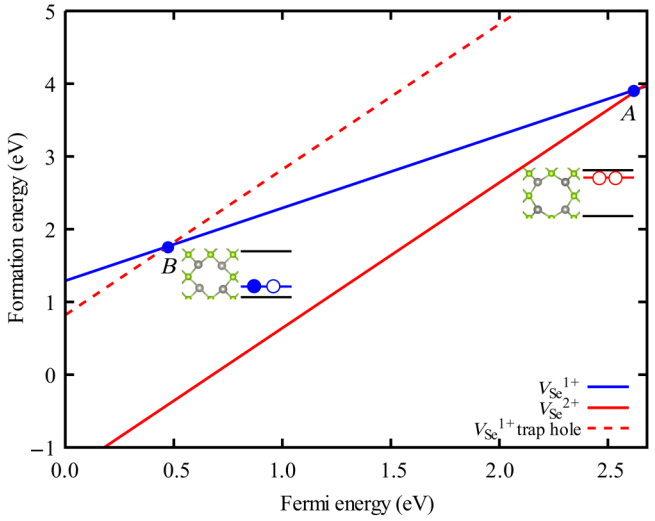

FIG. 4. HSE06-calculated formation energies of Se vacancy at 2+ and 1+ charge states in n-type ZnSe as functions of Fermi level (with reference to the VBM). Insets show atomic and electronic configurations under different charge states. Green balls are Se atoms and gray balls are Zn atoms.

use the phonon modes and electron-phonon coupling constants based on the initial states as an approximation within the harmonic phonon approximation. The first step in the nonradiative-recombination process is electron trapping, which occurs through the (+/2+) transition-energy level at point A with a value of 2.65 eV above the VBM, which is close to the CBM. After easily trapping an electron, the structure of the defect system is fully relaxed and becomes V_{Se}^+, as denoted by the solid blue line in Fig. 4. The second step is the hole-trapping process for fully relaxed V_{Se}^+ to trap a hole from the valence band at point B. The (+/2+) transition-energy level at point B is 0.49 eV above the VBM. After the V_{Se}^+ state trapping a hole and becoming a 2+ charge state, V_{Se}^{2+} exhibits a very large lattice relaxation, with a large reduction (2.18 eV) in its formation energy. Thus, the transition-energy level is pushed back to point A. Consequently, a cyclic nonradiative-recombination process through a two-level mechanism is formed [7]. We quantitatively calculate the carrier-capture-rate coefficients through these transition-energy levels for electrons and holes, as shown in Table I.

Figure 5 shows the formation energies of the Se vacancy in the neutral and 1+ charge states in n-type ZnSe ($\mu_{Zn} = 0$ eV), as a function of Fermi level. The defect transition levels for points C and D are 1.38 and 0.96 eV above the VBM, respectively. One can conclude that the dominant electron-trapping process may occur through defect levels at point C, and the hole-trapping process can occur through defect levels at points C and D. The first step of the nonradiative-recombination process is to trap a hole from the valence band and become the 1+ charge state, resulting

TABLE I. Calculated electron-capture-rate coefficients, B_n, and hole-capture-rate coefficients, B_p, through defect levels at points A, B, C, and D in Figs. 4 and 5. Calculated nonradiative decay probabilities, W_{ij} (s^{-1}), and relaxation energy, λ (eV), within the PWmat code are also listed.

	Electron trapping			Hole trapping		
	B_n (cm^3s^{-1})	λ (eV)	W_{ij} (s^{-1})	B_p (cm^3s^{-1})	λ (eV)	W_{ij} (s^{-1})
A	2.63×10^{-8}	2.18	$1.74 \times 10^{+13}$	7.85×10^{-34}	0.60	2.28×10^{-14}
B	...	...	...	6.85×10^{-6}	0.60	$4.52 \times 10^{+15}$
C	5.28×10^{-9}	0.91	$2.59 \times 10^{+15}$	9.54×10^{-13}	0.41	$6.30 \times 10^{+8}$
D	...	...	...	1.06×10^{-10}	0.41	$7.00 \times 10^{+10}$

in a hole-trapping process. After V_{Se}^0 traps a hole, the formation energy of the 1+ charge state is denoted by the blue dashed line shown in Fig. 5. Hole trapping occurs through a transition level at point D in Fig. 5, which is located at 0.96 eV above the VBM. After trapping a hole, the defect system fully relaxes to V_{Se}^+ and the four nearest zinc atoms around the vacancy move outward, as shown in Fig. 3. The total energy is reduced by 0.41 eV due to this lattice relaxation, thus the transition level is pushed upward to point C. Then, the second step can be carried out to trap an electron through a transition level at point C with a value of 1.38 eV above the VBM. When V_{Se}^+ traps an electron and becomes V_{Se}^0 again, the cyclic nonradiative-recombination process is completed. It should be noted that, due to the defect level of V_{Se}^+ (C point) being far away from the CBM, the electron-trapping rate should still be very small. According to the SRH model, there is another possible recombination process that may occur only through point C: first, V_{Se}^0 traps a hole and becomes V_{Se}^+ through the deep transition-energy level and, then, V_{Se}^+ traps an electron and becomes V_{Se}^0. All calculated electron- and hole-capture-rate coefficients are shown in Table I.

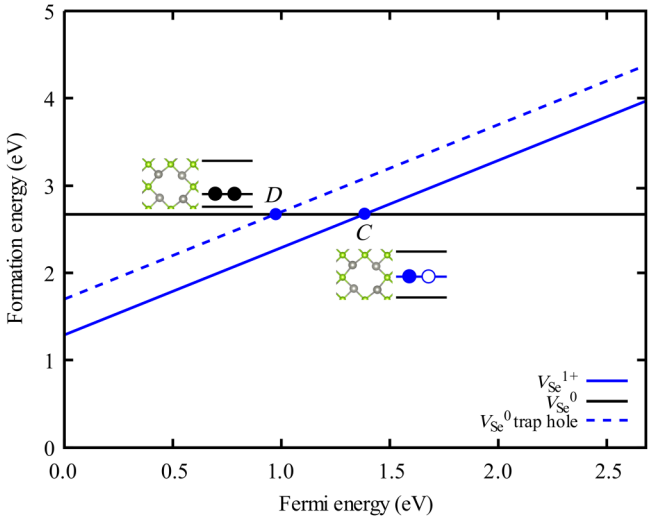

FIG. 5. HSE06-calculated formation energies of Se vacancy at neutral and 1+ charge states in n-type ZnSe as a function of Fermi level (with reference to the VBM). Insets show atomic and electronic configurations under different charge states. Green balls are Se atoms and gray balls are Zn atoms.

From the discussion and analysis above, we can summarize that the complete nonradiative-recombination process, through a two-level recombination mechanism, is most likely caused by V_{Se}^{2+} and V_{Se}^0. Based on the SRH model, the carrier recombination rate through only point C is lower than that of using points C and D. Because the hole-trapping rate (B_p) at point C is lower than that of point D by orders of magnitude, as shown in Table I. Meanwhile, it is noted that points A and B have a high electron-capture-rate coefficient, B_n, and a high hole-capture-rate coefficient, B_p, respectively. Hence, V_{Se}^{2+} has the possibility to be an effective recombination center in ZnSe under $\mu_{Zn} = -0.63$ eV conditions. Compared with the SRH model based on the single-defect level (point A or D), the nonradiative-recombination rate increases by several orders of magnitude through the two-level recombination mechanism based on points A and B. Therefore, the whole nonradiative-recombination process is mainly completed by V_{Se}^{2+} through points A and B. Actually, the electron-capture-rate coefficient is always large in the n-type semiconductors, and the enhancement of nonradiative recombination-process is mainly due to the increase of the hole-capture-rate coefficient. The large lattice relaxation that occurs in V_{Se}^{2+} is responsible for the high carrier-capture rates. This is because in the ionic group II-VI semiconductors, the defect level can shift from near the CBM (electron trapping) to near the VBM (hole trapping) due to large structural relaxation of the anion vacancy in different charged states caused by strong Coulomb interactions. Consequently, electrons can be trapped near the conduction band at a high rate, and then holes can be captured near the valence band at a high rate as well. For ionic semiconductors in group II-VI, large lattice relaxation often occurs in anion vacancies. We further confirm local atomic relaxations around the O vacancy in ZnO and the S vacancy in ZnS at the 2+, 1+, and neutral charged states, as shown in Fig. 6. Notably, the large lattice relaxation of the charged anion vacancies is also observed in

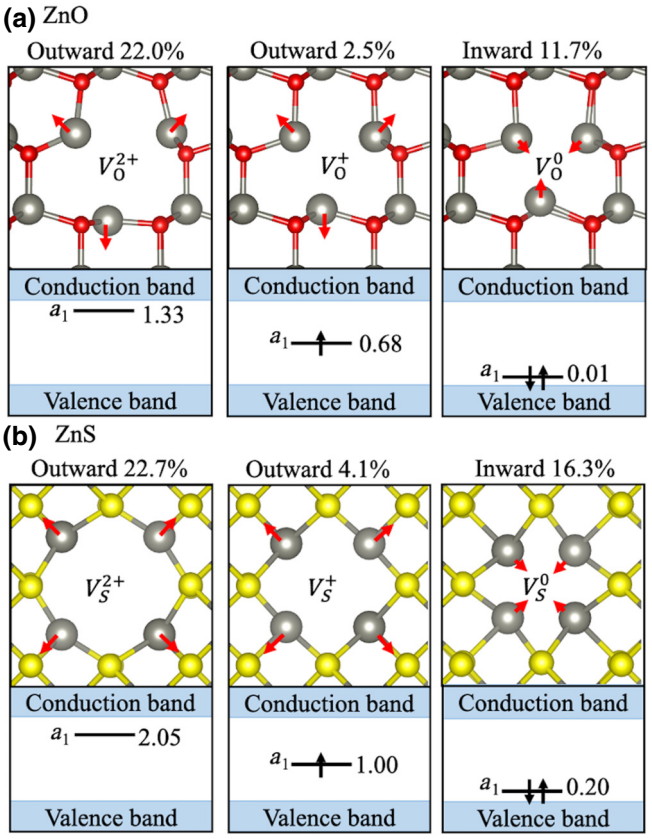

FIG. 6. Ball-and-stick representation of local atomic relaxations around (a) O vacancy in ZnO and (b) S vacancy in ZnS at 2+, 1+, and neutral charged states. Single-particle-level energies, with reference to the VBM, are also shown for each charge state. Gray balls are Zn atoms, red balls are O atoms, and yellow balls are S atoms.

ZnO and ZnS. For V_O^{2+} and V_S^{2+}, the nearest neighbors move outward by 22.0% and 22.7%, respectively, which is in good agreement with previous studies [40]. Since ZnO and ZnS belong to group II-VI semiconductors, they also have large lattice distortions caused by anion vacancies. Therefore, it may be possible to speculate that the nonradiative-recombination rate could be also enhanced in ZnO and ZnS by anion vacancies.

IV. CONCLUSIONS

We carefully analyze the nonradiative-recombination processes in group II-VI ionic semiconductors. For ZnX ($X = $ O, S, Se) systems, anion vacancies can bring out large lattice relaxations, resulting from strong Coulomb interactions between the nearest-neighboring atoms for different charged states, that largely increase the nonradiative-recombination rate. Therefore, our work provides an alternative way to demonstrate the nonradiative-recombination process in optoelectronic devices based on more ionic semiconductors.

ACKNOWLEDGMENTS

This work is supported by the National Key Research and Development Program of China (Grants No. 2020 YFB1506400 and No. 2018YFB2200100), the National Natural Science Foundation of China (Grants No. 61922077, No. 11874347, No. 11634003, and No. 11804333), and the Key Research Program of the Chinese Academy of Sciences (Grant No. XDPB22). H.-X.D. is also supported by the Youth Innovation Promotion Association of the Chinese Academy of Sciences (Grant No. 2017154).

[1] W. Shockley and W. T. Read, Statistics of the recombinations of holes and electrons, Phys. Rev. **87**, 835 (1952).
[2] R. N. Hall, Electron-hole recombination in germanium, Phys. Rev. **87**, 387 (1952).
[3] J. Nelson, *The Physics of Solar Cells* (Imperial College, London, 2003).
[4] A. M. Stoneham, Non-radiative transitions in semiconductors, Rep. Prog. Phys. **44**, 1251 (1981).
[5] H.-X. Deng, R. Cao, and S.-H. Wei, First-principles study of defect control in thin-film solar cell materials, Sci. China: Phys., Mech. Astron. **64**, 237301 (2021).
[6] L. Shi and L. W. Wang, Ab Initio Calculations of Deep-Level Carrier Nonradiative Recombination Rates in Bulk Semiconductors, Phys. Rev. Lett. **109**, 245501 (2012).
[7] J.-H. Yang, L. Shi, L. W. Wang, and S. H. Wei, Nonradiative carrier recombination enhanced by two-level process: A first-principles study, Sci. Rep. **6**, 21712 (2016).
[8] J.-H. Yang, W.-J. Yin, J.-S. Park, J. Ma, and S.-H. Wei, Review on first-principles study of defect properties of CdTe as a solar cell absorber, Semicond. Sci. Technol. **31**, 083002 (2016).
[9] J. Vanhellemont, P. Spiewak, K. Sueoka, and I. Romandic, On intrinsic point defect cluster formation during czochralski crystal growth, Phys. Status Solidi C **6**, 1906 (2009).
[10] G. D. Watkins, Intrinsic defects in silicon, Mater. Sci. Semicond. Process. **3**, 227 (2000).
[11] P. Śpiewak, J. Vanhellemont, K. Sueoka, K. J. Kurzydłowski, and I. Romandic, First principles calculations of the formation energy and deep levels associated with the neutral and charged vacancy in germanium, J. Appl. Phys. **103**, 086103 (2008).
[12] H.-X. Deng, J.-W. Luo, and S.-H. Wei, Band structure engineering and defect control of oxides for energy applications, Chin. Phys. B **27**, 117104 (2018).
[13] H.-X. Deng, S.-H. Wei, S.-S. Li, J. Li, and A. Walsh, Electronic origin of the conductivity imbalance between covalent and ionic amorphous semiconductors, Phys. Rev. B **87**, 125203 (2013).
[14] S. F. Chichibu, A. Uedono, K. Kojima, K. Koike, M. Yano, S.-i. Gonda, and S. Ishibashi, Hole capture-coefficient of intrinsic nonradiative recombination centers that commonly exist in bulk, epitaxial, and proton-irradiated ZnO, J. Appl. Phys. **127**, 215704 (2020).

[15] M. Berthe, R. Stiufiuc, B. Grandidier, D. Deresmes, C. Delerue, and D. Stievenard, Probing the carrier capture rate of a single quantum level, Science **319**, 436 (2008).
[16] L. Shi, K. Xu, and L.-W. Wang, Comparative study of ab initio nonradiative recombination rate calculations under different formalisms, Phys. Rev. B **91**, 205315 (2015).
[17] L. Shi, K. Xu, and L.-W. Wang, Reply to "Comment on 'Comparative study of ab initio nonradiative recombination rate calculations under different formalisms'", Phys. Rev. B **97**, 077302 (2018).
[18] L. Wang, Some recent advances in ab initio calculations of nonradiative decay rates of point defects in semiconductors, J. Semicond. **40**, 091101 (2019).
[19] Y. Xiao, Z. Wang, L. Shi, X. Jiang, S. Li, and L. Wang, Anharmonic multi-phonon nonradiative transition: An ab initio calculation approach, Sci. China: Phys., Mech. Astron. **63**, 277312 (2020).
[20] PWmat, http://www.pwmat.com
[21] S. S. Schmidt, D. Abou-Ras, S. Sadewasser, W. Yin, C. Feng, and Y. Yan, Electrostatic Potentials at Cu(In, Ga)Se_2 Grain Boundaries: Experiment and Simulations, Phys. Rev. Lett. **109**, 095506 (2012).
[22] W. Jia, J. Fu, Z. Cao, L. Wang, X. Chi, W. Gao, and L.-W. Wang, Fast plane wave density functional theory molecular dynamics calculations on multi-GPU machines, J. Comput. Phys. **251**, 102 (2013).
[23] W. Jia, Z. Cao, L. Wang, J. Fu, X. Chi, W. Gao, and L.-W. Wang, The analysis of a plane wave pseudopotential density functional theory code on a GPU machine, Comput. Phys. Commun. **184**, 9 (2013).
[24] J. Heyd, G. E. Scuseria, and M. Ernzerhof, Hybrid functionals based on a screened Coulomb potential, J. Chem. Phys. **118**, 8207 (2006).
[25] H. Li and W. Jie, Growth and characterizations of bulk ZnSe single crystal by chemical vapor transport, J. Cryst. Growth **257**, 110 (2003).
[26] H. J. Monkhorst and J. D. Pack, Special points for brillouin-zone integrations, Phys. Rev. B **13**, 5188 (1976).
[27] S.-H. Wei, Overcoming the doping bottleneck in semiconductors, comp. Mater. Sci. **30**, 337 (2004).
[28] S. B. Zhang and J. E. Northrup, Chemical Potential Dependence of Defect Formation Energies in GaAs: Application to Ga Self-Diffusion, Phys. Rev. Lett. **67**, 2339 (1991).
[29] J. Ma, S.-H. Wei, T. A. Gessert, and K. K. Chin, Carrier density and compensation in semiconductors with multiple dopants and multiple transition energy levels: Case of Cu impurities in CdTe, Phys. Rev. B **83**, 245207 (2011).
[30] W. J. Schutte, J. L. De Boer, and F. Jellinek, Crystal structures of tungsten disulfide and diselenide, J. Solid State Chem. **70**, 207 (1987).
[31] J. L. Merz, H. Kukimoto, K. Nassau, and J. W. Shiever, Optical properties of substitutional donors in ZnSe, Phys. Rev. B **6**, 545 (1972).
[32] D. Krasikov, A. Knizhnik, B. Potapkin, and T. Sommerer, Why shallow defect levels alone do not cause high resistivity in CdTe, Semicond. Sci. Technol. **28**, 125019 (2013).
[33] J.-H. Yang, J.-S. Park, J. Kang, and S.-H. Wei, First-principles multiple-barrier diffusion theory: The case study of interstitial diffusion in CdTe, Phys. Rev. B **91**, 075202 (2015).
[34] R. Pässler, Description of nonradiative multiphonon transitions in the static coupling scheme, Czech. J. Phys. **24**, 322 (1974).
[35] R. Pässler, Nonradiative multiphonon transitions described by static versus adiabatic coupling scheme in comparison with Landau-Zener's theory, Czech. J. Phys. **32**, 846 (1982).
[36] K. Huang, Lattice relaxation and multiphonon transitions, Contemp. Phys. **22**, 599 (1981).
[37] D. B. Laks, C. G. Van De Walle, G. F. Neumark, P. E. Blochl, and S. T. Pantelides, Native defects and self-compensation in ZnSe, Phys. Rev. B **45**, 10965 (1992).
[38] J. Mimila and R. Triboulet, Sublimation and chemical vapor transport, a new method for the growth of bulk ZnSe crystals, Mater. Lett. **24**, 221 (1995).
[39] A. Garcia and J. E. Northrup, Compensation of p-Type Doping in ZnSe: The Role of Impurity-Native Defect Complexes, Phys. Rev. Lett. **74**, 1131 (1995).
[40] A. Janotti and C. G. Van de Walle, Oxygen vacancies in ZnO, Appl. Phys. Lett. **87**, 122102 (2005).
[41] J. E. Northrup and S. B. Zhang, Energetics of the as vacancy in GaAs: The stability of the 3+ charge state, Phys. Rev. B **50**, 4962 (1994).